Quantum Chemical Study on Corrosion Inhibition Efficiency of 4-amino-5-mercapto-1,2,4-triazole Derivatives for Copper in HCl Solution

Ephrem G. Demissie, Solomon B. Kassa, Girma W. Woyessa

Abstract— The inhibition of copper corrosion by three 4-amino-5-mercapto-1,2,4-triazole derivatives was studied theoretically using hybrid DFT functional (B3LYP/6-31G (d,p)). The chemical reactivity descriptors, such as electronegativity, global hardness, softness, electrophilicity, E_{HOMO}, E_{LUMO}, dipole moment, $\Delta E_{Back\text{-}donation}$, Fukui functions of the investigated inhibitor computed from density functional theory were reported in this paper. In addition, Nucleus independent Chemical Shift Analysis (NICS) were introduced to further study the aromaticity parameter to describe the reactivity of these inhibitors at the Cu surface. The studies have shown that, 4-amino-3-ethyl-5-mercapto-1,2,4-triazole (AEMT) is the most efficiency inhibitor than 4-amino-5-mercapto-1,2,4-triazole (AMT) and 4-amino-3-methyl-5-mercapto-1,2,4-triazole (AMMT) for copper in HCl medium. The theoretical work was consistent with the experimentally obtained result.

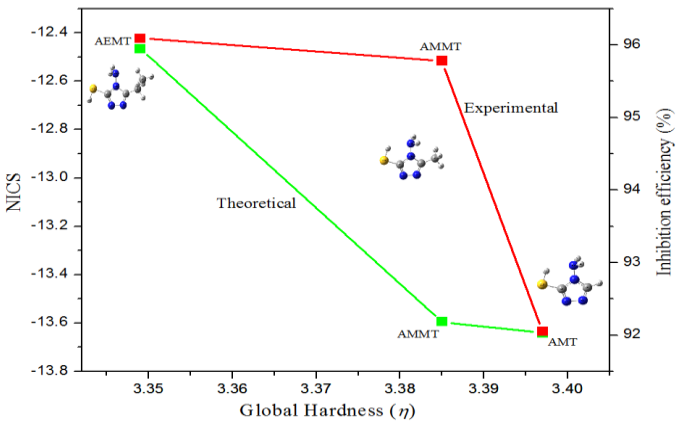

Schematically representation of the inhibition efficiency of 4-amino-5-mercapto-1,2,4-triazole derivatives

Index Terms— DFT method, NICS, Chemical reactivity descriptors, AMT, AMMT, AEMT

1. Introduction

Copper is one of the most essential metals widely used electrical and thermal conductivities in manufacture such as electronics and in the integrated circuits. It also used in different industries, especially in central heating installations, car industry, oil refineries, sugar factories, and so on [1-3]. Copper and its alloys are good corrosion resistance in water and have excellent heat conductivity, but these corrode easily in acid such as hydrochloric acid solutions. It is generally a relatively noble metal, however, it is susceptible to corrosion by acids and strong alkaline solutions, especially in the presence of oxygen or oxidants [4,5]. The inhibition properties of these reactions can be controlled by many types of organic and inorganic compounds, but organic compounds are the more common type of corrosion inhibitors [5-7].

- *Ephrem G. Demissie, Haramaya University, Department of Chemistry, Ethiopia, E-mail: ephrem1977@gmail.com*
- *Solomon B. Kassa, Haramaya University, Department of Chemistry, Ethiopia, E-mail: solomon.bezabeh72@gmail.com*
- *Girma W. Woyessa, Haramaya University, Department of Chemistry, Ethiopia, E-mail: abelgirma827@gmail.com*

The most efficient inhibitors are organic compounds having π bonds in their structures. The efficiency of an organic compound as a successful inhibitor is mainly dependent on its ability to get adsorbed on the metal surface. The process of adsorption is influenced by the metal surface, the chemical structure of the organic inhibitor, the distribution of charge in the molecule, the type of aggressive electrolyte and the type of interaction between organic molecules and the metallic surface [8-11]. The role of adsorption-type inhibitors of heteroatoms containing organic compounds, such as P, S, N, and O, having lone pair of electrons can be explained by the Lewis acid-base interaction. The heteroatoms may interact with the metal substrate through an electron donation mechanism, reducing metal dissolution at the metal-electrolyte interface [5,12].

Many substituted triazoles have recently been studied in much detail as effective corrosion inhibitors for copper in acidic media [13-15]. Triazole and its derivatives are also found associated with various biological Activities. They possess wide spectrum of activities ranging from anti-bacterial, anti-inflammatory, anticonvulsant, anti-neoplastic, antimalarial, antiviral, anticancer [16-18]. The molecular

structure of triazoles and its derivatives contain atoms like N and S, which are easily able to bridge with other molecules. Nitrogen and sulphur-containing triazoles and its derivative compounds may act as inhibitors for copper dissolution due to the chelating action of heterocyclic molecules and the formation of a physical blocking barrier on the copper surface [1,4,19,20].

The inhibitive properties of three different triazole derivatives namely, 4-amino-5-mercapto-1,2,4-triazole (AMT), 4-amino-3-methyl-5-mercapto-1,2,4-triazole (AMMT), and 4-amino-3-ethyl-5-mercapto-1, 2, 4-triazole (AEMT) have been reported [16]. A perusal of literature reveals that corrosion efficiency of AEMT > AMMT > AMT have not been reported using quantum chemical calculations. The present work investigate the inhibition efficiency of these compounds based on theoretical studies using chemical reactivity descriptors such as energy of highest occupied molecular orbital (E_{HOMO}), energy of lowest unoccupied molecular orbital (E_{LUMO}), energy gap (ΔE), dipole moment (μ), electronegativity (χ), electron affinity (A), global hardness (η), softness (σ), ionization potential (I), the global electrophilicity (ω), the fraction of electrons transferred (ΔN), chemical potential (μ), $\Delta E_{Back\text{-}donation}$, and Nucleus independent Chemical Shift Analysis (NICS). Fig. 1 shows the Lewis structures of the investigated 4-amino-5-mercapto-1,2,4-triazole derivatives.

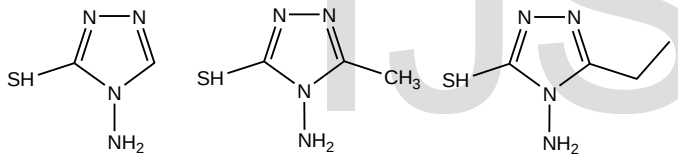

AMT AMMT AEMT

Fig. 1 Molecular structure of 4-amino-5-mercapto-1,2,4-triazole derivatives.

2. Methodology

Density Functional Theory (DFT) methods were employed to study the inhibition efficiency 4-amino-5-mercapto-1,2,4-triazole derivatives. Among quantum chemical methods for evaluation of corrosion inhibitors, density functional theory (DFT) has shown significant promise and appears to be adequate for pointing out the changes in electronic structure responsible for inhibitory action [21]. In addition, DFT methods become very popular due to their accuracy that is similar to other methods in less time and with a smaller investment from the computational point of view. In DFT, the energy of the fundamental state of a polyelectronic system can be expressed as the total electronic density, and, in fact, use of electron density instead of a wave function for calculating the energy constitutes the fundamental basis of DFT [2,22].

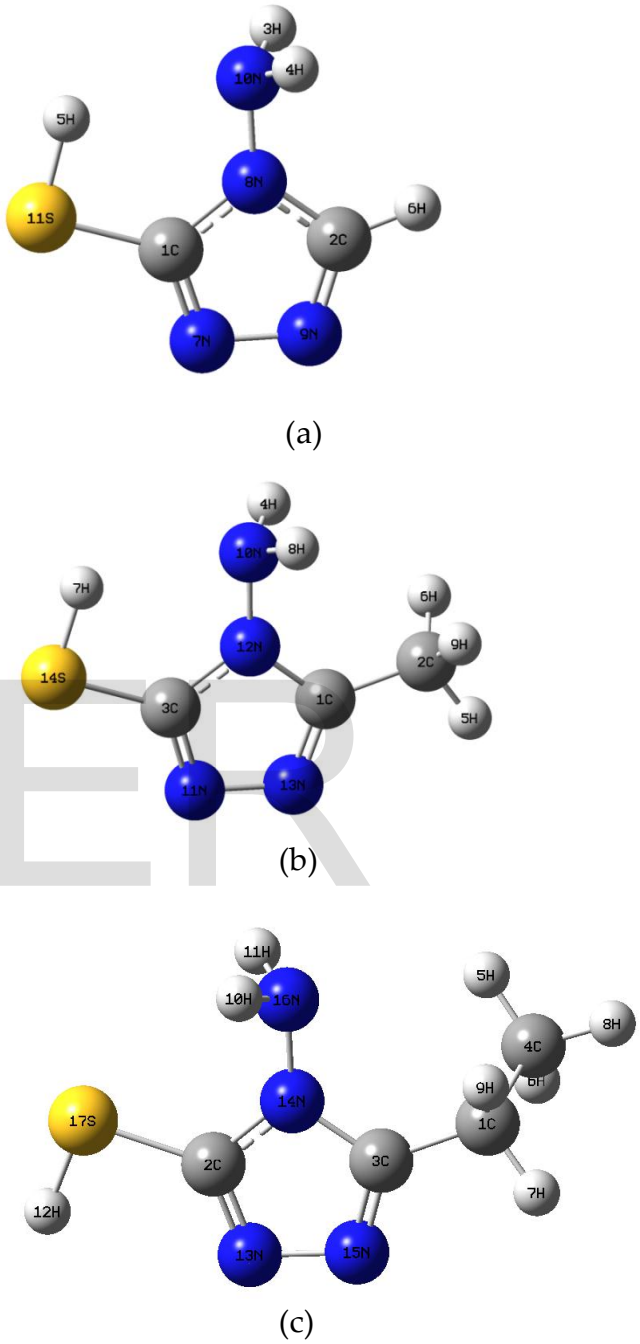

Fig. 2 Optimized molecular structure of (a) AMT, (b) AMMT and (c) AEMT by B3LYP/6-31G (d,p)

Geometry optimizations of ground state at DFT level, with the hybrid B3LYP exchange-correlation function and the split valence 6-31G (d,p) basis set were carried out without imposing constraint as implemented in Gaussian 09W [23].

The optimized molecular structures of the molecules studied, obtained based on the hybrid DFT functional (B3LYP/6-31G (d,p)) were shown in Fig. 2.

3. Result and Discussion

3.1. Theoretical calculation

The quantum chemical calculations have been widely used to study the reaction mechanisms and to interpret the experimental results as well as to solve chemical ambiguities [24]. The recent progress in DFT has provided a very useful tool for understanding molecular properties and for describing the behavior of atoms in molecules [2]. The basic relationship of the density functional theory of chemical reactivity is precisely, the one established by Parr, Donnelly, Levy and Palke, that links the electronic chemical potential μ with the first derivative of the energy with respect to the number of electrons, which in a finite difference version is given as the average of the ionization potential (I) and electron affinity (A), and therefore with the negative of the electronegativity χ [25].

$$-\mu = \chi = \frac{\partial E}{\partial N_{elec}} \approx \frac{I + A}{2} \qquad 1.$$

Electronegativity has also been expressed in terms of orbital energies [26]. According to Koopman's theorem, E_{HOMO} and E_{LUMO} of the inhibitor molecule are related to the ionization potential (I) and the electron affinity (A), respectively, i.e. by taking I as the negative of the HOMO energy and A as the negative of the LUMO energy [24,27]. This gives

$$\chi = \frac{-(E_{HOMO} + E_{LUMO})}{2} \qquad 2.$$

The second derivative of the energy with respect to the number of electrons is the hardness η [28], which again can be approximated in terms of ionization potential (I) and the electron affinity (A) of the inhibitor molecule.

$$\eta = \frac{1}{2}\frac{\partial^2 E}{\partial N_{elec}^2} = \frac{I - A}{2} \qquad 3.$$

Global softness (σ) is the reciprocal of global hardness [29]. From Eq. (3) it becomes:

$$\sigma = \frac{1}{\eta} = \frac{2}{I - A} \qquad 4.$$

The electrophilicity index measures the electrophilic power of a molecule [2,30]. This parameter, is defined as

$$\omega = \frac{\chi^2}{2\eta} \approx \frac{(I + A)^2}{4(I - A)} \qquad 5.$$

According to Pearson theory [31], the number of electrons transferred (ΔN) can be calculated depending on the quantum chemical method. The values of ΔN show inhibition effect resulted from electrons donation

$$\Delta N = \frac{\chi_{Cu} - \chi_{inh}}{2\sum \eta_{Cu} + \eta_{inh}} \qquad 6.$$

where χ_{Cu} and χ_{inh} denotes the absolute electronegativity of copper and the inhibitor molecule, respectively; η_{Cu} and η_{inh} denotes the absolute hardness of copper and the inhibitor molecule, the absolute electronegativity, χ, and absolute hardness, η is a chemical property that describes the ability of a molecule to attract electron towards itself in a covalent bond [32]. Therefore, the difference in electronegativity drives the electron transfer, and the sum of the hardness parameters acts as a resistance [1].

The local reactivity of the molecules was analyzed through an evaluation of the Fukui function was introduced by Parr and Yang [33]. This function used as a measurement of changes in electron density that accompanies chemical reactions; indicative of the reactive regions, that is, the nucleophilic and electrophilic behavior of the molecule. Calculations are based on the finite difference approximations and partitioning of the electron density (r) between atoms in a molecular system [34]. The change in electron density is the nucleophilic $f^+(r)$ and electrophilic $f^-(r)$ Fukui functions, which can be calculated using the finite difference approximation as follows

$$f^+(r) = q_{N+1} - q_N \qquad 7.$$

$$f^-(r) = q_N - q_{N-1} \qquad 8.$$

where q_N, q_{N+1} and q_{N-1} are the electronic population of the atom k in neutral, anionic and cationic systems. Condensed softness indices allowing the comparison of reactivity between similar atoms of different molecules can be calculated easily starting from the relation between the Fukui function $f(r)$ and the local softness $s(r)$ [21]

$$s(r) = \left(\frac{\partial \rho(r)}{\partial N}\right)_{V(r)} \left(\frac{\partial N}{\partial \mu}\right)_{V(r)} = f(r)S \quad 9.$$

3.2. Correlation between Molecular Orbital Energy Level and Inhibition Efficiency

The inhibition of copper has been investigated experimentally using AMT, AMMT, and AEMT as corrosion inhibitors [16] and the result presented in Table 1. The calculated values of E_{HOMO}, E_{LUMO}, dipole moment and energy gap of the investigated inhibitor from Gaussian 09 using DFT/B3LYP given in Table 2.

Table 1 Parameters obtained experimentally for copper in 0.5M HCl solutions in the absence and presence of (a) AMT (b) AMMT (c) AEMT at 303 K temperature.

Acid solution	Conc. of inhibitor (mol L^{-1})	Inhibition efficiency (%)
0.5 M HCl	-	-
AMT	8.26×10^{-4}	84.39
	1.72×10^{-3}	87.94
	2.58×10^{-3}	92.05
AMMT	8.26×10^{-4}	91.56
	1.72×10^{-3}	92.96
	2.58×10^{-3}	95.78
AEMT	8.26×10^{-4}	90.54
	1.72×10^{-3}	93.70
	2.58×10^{-3}	96.09

According to the frontier molecular orbital theory of chemical reactivity, transition of electron is due to interaction between highest occupied molecular orbital (HOMO) and lowest unoccupied molecular orbital (LUMO) of reacting species [25]. The deeper reason is that the shapes of the HOMO and LUMO resemble features in the total electron density, which determines the reactivity. The energy of highest occupied molecular orbital measures the tendency of the inhibitor to donate the electron. The adsorption of the inhibitor on the metal surface can occur on the basis of donor–acceptor interactions between the π-electrons of the heterocyclic compound and the vacant d-orbital of the metal surface atoms [24].

With increasing the energy of E_{HOMO} of the inhibitor the electrons can jump easily to the metal surface, which in turn enhancing the adsorption of the inhibitor on copper metal and therefore better inhibition efficiency. E_{LUMO} indicates the ability of the molecules to accept electrons. The lower value of E_{LUMO}, the more probable the molecule accepts electrons. The E_{HOMO} values show that AEMT and AMMT have good electron donor properties compared to AMT. This is due to the presence of ethyl and methyl in the five member ring of AEMT and AMT respectively. Ethyl and methyl groups in AEMT or AMT increases the electron density on sulfur and nitrogen as shown in Fig. 2, and can be donated easily for adsorption and bonding on the copper surface.

Table 2 Global chemical reactivity indices for AMT, AMMT and AEMT calculated using B3LYP/6-31G (d,p) in aqueous solution.

Parameters	AMT	AMMT	AEMT
Total energy (a.u)	-695.778	-735. 104	-774.419
E_{HOMO} (eV)	-6.442	-6.318	-6.306
E_{LUMO} (eV)	0.352	0.450	0.392
Energy gap (eV)	6.794	6.769	6.698
Dipole Moment (D)	9.4871	9.7572	9.7767

Even if survey of the literature reveals that several irregularities appeared in the case of the correlation of dipole moment with inhibitor efficiency [35], for the dipole moment (μ), higher values will favorite enhancement of corrosion inhibition [36]. The dipole moment of AEMT is higher than that of AMMT and AMT, as a result of the stronger electron-donating effect of ethyl in AEMT. And because of that, a correlation between the dipole moments of the molecules and inhibition efficiency were observed. The energy gap between the E_{HOMO} and E_{LUMO} energy levels of the molecules was another important factor that should be considered. A large E_{HOMO}-E_{LUMO} gap implies high stability for the molecule in chemical reactions and, a decrease of the energy gap usually leads to easier polarization of the molecule as well as adsorption on the surface [37]. The smaller value of energy gap in AEMT causes higher inhibition efficiencies of Cu metal. In general from Table 2, it can be clearly seen that the inhibition efficiency based on the E_{HOMO}, energy gap and the dipole moment for three compounds followed the order of AEMT > AMMT > AMT. This was in a good agreement with the experimentally determined inhibition efficiency

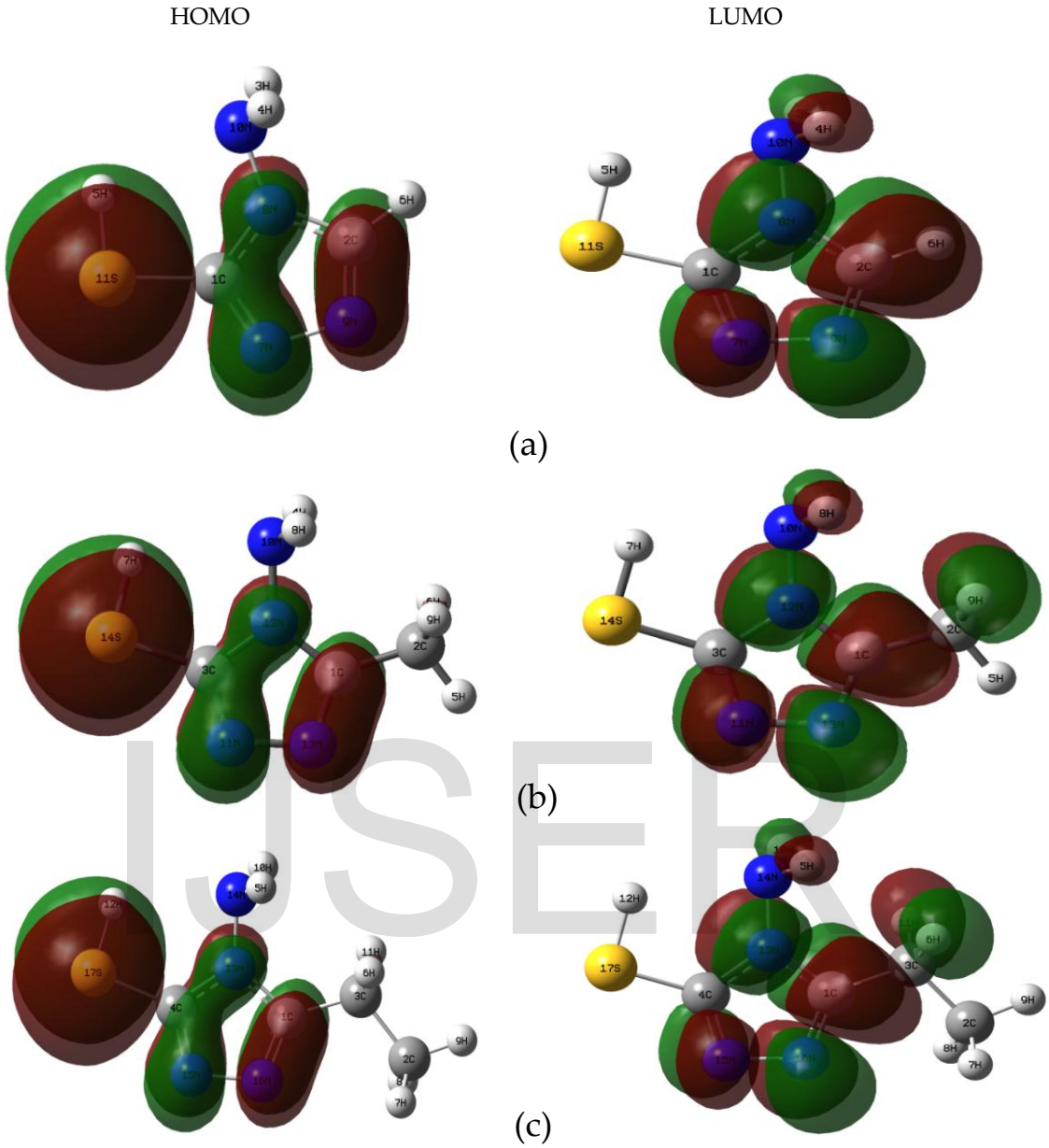

Fig. 3 The frontier molecular orbital (HOMO-LUMO) density distributions of 4-amino-5-mercapto-1, 2, 4-triazole derivatives (a) AMT, (b) AMMT and (c) AEMT

3.3. Global chemical reactivity

Ionization energy and electron affinity are fundamental descriptor of the chemical reactivity of atoms and molecules. High ionization energy indicates high stability and chemical inertness and small ionization energy indicates high reactivity of the atoms and molecules [31]. As shown in Table 3, the low ionization energy 6.305 (eV) of AEMT indicates the high inhibition efficiency. Absolute hardness and softness are also important properties to measure the global chemical reactivity and molecular stability. It is apparent that the chemical hardness fundamentally signifies the resistance towards the deformation or polarization of the electron cloud of the atoms, ions or molecules under small perturbation of chemical reaction. A hard molecule has a large energy gap and a soft molecule has a small energy gap [25]. As can be seen clearly from Table 3, AEMT with lowest hardness (highest softness) value signifies high reactivity toward copper metal and better inhibition.

Table 3 Quantum chemical descriptors for AMT, AMMT and AEMT calculated using B3LYP/ 6-31G (d,p) in aqueous solution.

Parameters/ (eV)	AMT	AMMT	AEMT
Ionization Energy (I)	6.442	6.318	6.305
Electron Affinity (A)	-0.352	-0.450	-0.392
Global Hardness (η)	3.397	3.385	3.349
Electronegativity (χ)	3.045	2.934	2.957
Electrophilicity (ω)	1.365	1.272	1.305
Chemical potential (μ)	-3.045	-2.934	-2.957
Global Softness (S)	0.294	0.295	1.305
Transferred electrons fractions (ΔN)	0.285	0.302	0.305
$\Delta E_{Back\text{-}donation}$	-0.849	-0.846	-0.837

From Table 3, it is possible to observe that molecule AEMT has lowest absolute electonegativity (highest chemical potential) in turn, is AMMT then AMT. Electronegativity is a measure of how hospitable an atom or a group of atom in a molecule is to the access of electronic charge. With lowest electonegativity and highest chemical potential, AEMT has better inhibition efficiency.

When copper and inhibitor are brought together, electrons will flow from lower potential (inhibitor) to higher potential (Cu), until the chemical potential becomes equal. The fraction of electrons transferred ΔN, theoretically calculated by taking the absolute electronegativity of copper according to Pearson Cu = 4.98 eV, and a global hardness of η_{Cu} = 0, by assuming that for a metallic bulk I = A, because they are softer than the neutral metallic atoms [1]. According to Lukovits's study, if the value of ΔN < 3.6, the inhibition efficiency increased with increasing electron donating ability of inhibitor at the metal surface [37]. In our case inhibition efficiency also increased with increase in the values of ΔN. Thus, the highest fraction of electrons transferred is associated with the best inhibitor (AEMT), while the least fraction is associated with the inhibitor that has the least inhibition efficiency (AMT). In Table 3, the calculated $\Delta E_{Back\text{-}donation}$ values for the inhibitors also listed. According to Gomeze et al. [38], during the presence of charge transfer the back donation of charges is the negative of hardness (-η/4) which governing the interaction between the inhibitor molecule and the metal surface. The $\Delta E_{Back\text{-}donation}$ implies that when η > 0 and $\Delta E_{Back\text{-}donation}$ < 0 the charge transfer to a molecule, followed by a back-donation from the molecule, is energetically favored [39]. Hence, the order followed is: AEMT > AMMT > AMT, which indicates that back donation, is favoured for the AEMT, which is the best inhibitor. Other parameters such as the electrophilicity (ω) which measures the total ability to attract electrons also asserts the mentioned facts.

Therefore, according to a series of properties calculated for each molecule shown in Table 3, the inhibitive effectiveness orders for the molecules are: AEMT > AMMT > AMT. The theoretical calculated values were consistent with the experimentally obtained result.

3.4. Local chemical reactivity

The energy levels of frontier orbitals indicate the tendency to form bonds to the metal surface [40]. Further study on the spatial distribution of the electron density of inhibitors, i.e. the local concentration and local depletion of electron charge density allows us to determine whether the inhibitor undergo electrophilicity or nucleophilicity reaction [41]. To examine the local reactivity behavior we have calculated the Fukui function and local softness indices from Mulliken charge, which summarized in Table (4 and 6). Parr and Yang proposed that larger value of Fukui function indicate more reactivity. Hence greater the value of condensed Fukui function, the more reactive is the particular atomic centre in the molecule [31]. The highest value f_k^+ and s_k^+ for AMT, AMMT, and AEMT occurs at S11, S14, and S17 respectively, indicating that sulfur atom as can be seen in the electron density cloud in Fig. 3, will donate charge when attacked by an electrophilic reagent. While N 7, N 11, and N 13 were the most reactive site based on f_k^- and s_k^- for nucleophilic attack in the compound AMT, AMMT, and AEMT respectively.

Table 4 Fukui and local softness indices for AMT atoms calculated from Mulliken atomic charges.

Atom No	f_k^+	f_k^-	s_k^+	s_k^-
1 C	0.03747	0.05936	0.01102	0.01745
2 C	0.10138	0.02988	0.02981	0.00879
3 H	0.07237	-0.01548	0.02128	-0.00455
4 H	0.07269	-0.01647	0.02137	-0.00484
5 H	0.13289	0.00787	0.03907	0.00231
6 H	0.13868	-0.02775	0.04077	-0.00816
7 N	**0.17846**	0.12829	**0.05247**	0.03772
8 N	0.04491	-0.02263	0.01320	-0.00665
9 N	0.03030	0.12065	0.00891	0.03547
10 N	-0.01216	0.02941	-0.00357	0.00865
11 S	0.10299	**0.20685**	0.03028	**0.06081**

Table 5 Fukui and local softness indices for AMMT atoms calculated from Mulliken atomic charges.

Atom No	f_k^+	f_k^-	s_k^+	s_k^-
1 C	0.06163	0.00615	0.01818	0.00182
2 C	-0.01220	-0.02821	-0.00360	-0.00832
3 C	0.00427	0.04914	0.00126	0.01450
4 H	0.04357	0.04345	0.01285	0.01282
5 H	0.05427	0.05829	0.01601	0.01720
6 H	0.06502	0.01253	0.01918	0.00370
7 H	0.05571	0.05170	0.01644	0.01525
8 H	0.04356	-0.00059	0.01285	-0.00017
9 H	0.06505	0.03101	0.01919	0.00915
10 N	0.00540	0.01622	0.00159	0.00479
11 N	**0.23993**	0.06067	**0.07078**	0.01790
12 N	0.02042	-0.01277	0.00602	-0.00377
13 N	0.11652	0.06571	0.03437	0.01938
14 S	0.13686	**0.44672**	0.04037	**0.13178**

Table 6 Fukui and local softness indices for AEMT atoms calculated from Mulliken atomic charges.

Atom No	f_k^+	f_k^-	s_k^+	s_k^-
1 C	-0.03955	-0.01092	-0.05161	-0.01425
2 C	0.02305	0.12513	0.03008	0.16329
3 C	0.05713	0.14239	0.07455	0.18582
4 C	-0.01025	-0.03184	-0.01338	-0.04155
5 H	0.06306	0.01687	0.08229	0.02201
6 H	0.01679	0.05571	0.02191	0.07270
7 H	-0.00517	0.07707	-0.00675	0.10058
8 H	0.05575	0.06265	0.07275	0.08176
9 H	0.08655	0.03268	0.11295	0.04264
10 H	0.02416	0.15628	0.03152	0.20394
11 H	0.04165	0.08688	0.05435	0.11338
12 H	0.04174	0.11428	0.05447	0.14914
13 N	**0.13218**	0.02965	**0.17249**	0.03870
14 N	0.02447	-0.00904	0.03194	-0.01180
15 N	0.11909	0.02686	0.15542	0.03506
16 N	-0.00853	-0.01658	-0.01113	-0.02164
17 S	0.11789	**0.14194**	0.15385	**0.18524**

3.5. Vibrational mode

AMT has 11 atoms with 27 normal modes of vibration while AMMT has 14 atoms with 36 normal modes of vibrations and AEMT has 17 atoms with 45 vibration mode. On the basis of our calculations and the reported FT-IR spectra [16], we made a reliable one-to-one correspondence between the fundamentals and the frequencies calculated by DFT (B3LYP, 6-31(d,p)) methods. The theoretical vibrational spectra scaled by 0.9613 have been multiplied to the final obtained values presented in Table 7. The assignments of the calculated frequencies are aided by the animation option of Gaussian program.

Table 7 Comparison of experimental FT-IR spectra with calculated vibrational wave numbers (cm^{-1}) with B3LYP/6-31G (d, p) basis set

Compounds	Parameters	Exp. data	Theoretical values B3LYP/6-31G (d, p)
AMT	NH_3	3392	3350(sym), 3443(asym)
	CH (ring)	3250	3140
	SH	2380	2564
	C=N	1600	1474
	N-N		988
AMMT	NH_2	3400	3345(sym), 3436(asym)
	CH-(CH_3)	3246	2917(sym), 3038(asym)
	SH	2392	2561
	C=N	1612	1527
	N-N		1025
AEMT	NH_2	3396	3343(sym), 3433(asym)
	CH_2	3236	3065(sym), 3150(asym)
	SH	2382	256
	C=N	1608	1520
	N=N		1025

The DFT values were found to be in good agreement with the experimental values after scaling the vibrational frequencies. As can be clearly seen in Table 7 from the experimental result the theoretical value of the vibrational frequency further validate the reliability of using DFT (B3LYP/6-31(d,p)) to estimate the relative corrosion efficiency of AMT, AMMT, and AEMT.

3.6. Nucleus independent chemical shift (NICS) Analysis

The nucleus-independent chemical shift (NICS) method has been widely employed to characterize aromaticity [42] from the magnetic point of view. The index is defined as the negative value of the absolute magnetic shielding computed at the ring center or another interesting point of the system. Rings with highly negative values of NICS are quantified as aromatic by definition, whereas those with positive values are anti-aromatic [43].

Table 8 NICS values calculated at the ring center and 0.5 & 1.0 Å above the ring along the Z-axis

compounds	NICS (0)	NICS (0.5)	NICS (1)
AMT	-11.7973	-13.6412	-12.8843
AMMT	-11.3578	-13.5948	-12.6789
AEMT	-11.0255	-12.4657	-12.0238

NICS values calculated along the *z*-axis to the benzene ring plane beginning on the center of the ring up to 1.0 Å using DFT (B3LYP, 6-31(d,p)) given in Table 8. For all molecule the highest absolute value obtained above the ring at the distance of 0.5 Å. The aromaticity value along the Z-direction on the center of the ring for all possible value increases in the order of AMT > AMMT>AEMT. Furthermore, as can be clearly seen from Fig. 4 the aromaticity has linearly increases with global hardness. On the basis of aromaticity test using NICS, with decreasing aromaticity the reactivity of the molecule increased. Therefore, AEMT was less aromatic and has the highest corrosion inhibition efficiency.

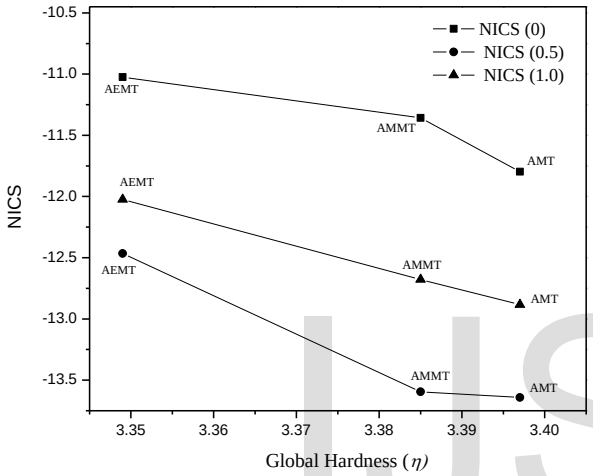

Fig. 4 A linear correlation between NICS and global hardness for AMT, AMMT, and AEMT

4. Conclusion

The present study on the inhibition efficiency 4-amino-5-mercapto-1,2,4-triazole derivatives has lead us AEMT was the most efficient inhibitor for copper metal in HCl medium. The chemical reactivity descriptors, such as electronegativity, global hardness, softness, electrophilicity, E_{HOMO}, dipole moment, $\Delta E_{Back\text{-}donation}$, transferred electrons fractions has shown that the inhibition efficiency follows the order AEMT > AMMT > AMT. Our calculations using Fukui function and local softness indices predicted the nucleophilic and electrophilic attacking sites of the inhibitors. The NICS results suggest that the order of aromaticity of the inhibitor was AMT > AMMT >AEMT, which is inversely proportional to reactivity of the molecule. In general, the results obtained from quantum chemical calculations were in good agreement with the experimental studies.

Acknowledgment: Many thanks due to Mr. Birhanu Haile

Reference

[1] K.F. Khaled, (2010), Corrosion Science, 52, 3225–3234
[2] P. M. Niamien, H. A. Kouassi, A. Trokourey, F. K. Essy, D. Sissouma, and Y. Bokra, (2012), Materials Science, 1-15
[3] K. Barouni, A. Kassale, A. Albourine, O. Jbara, B. Hammouti, L. Bazzi, (2014), J. Mater. Environ. Sci. 5 (2), 456-463,
[4] Gy. Vastag, E. Szöcs, A. Shaban, and E. Kálmán, (2001), Pure Appl. Chem., 73, (12), 1861–1869
[5] Fatemeh Baghaei Ravari, Athareh Dadgarinezhad, Iran Shekhshoaei, (2009), G.U. J. Sci., 22(3), 175-182
[6] Mehdi Ebadi, Wan Jeffrey Basirun, Hamid Khaledi and Hapipah Mohd Ali, (2012), Chemistry Central Journal, 6:163-172
[7] M. M. Antonijevic, M. B. Petrovic, Int. J. Electrochem. Sci., 3, 2008, 1-28,
[8] Lagrenee M, Mernari B, Bouanis M, Traisnel M, Bentiss F, (2000), Corros Sci., 44(3), 573-588.
[9] Bentiss F, Lagrenee M, Traisnel M, Hornez J.C, Corrs Sci., 41(4),1999, 789-803
[10] El-Sayed, M. Sherif, (2006) Applied surface science, 252, 8615-8623
[11] R.Subramanian, V. Lakshminarayanan, (2002), Corrosion Science, 44, 535
[12] S. S. Shivakumar and K. N.Mohana, (2013) International Journal of Corrosion, 1-13
[13] Y. Ahmed, A.A.H. Kadhum, A.B. Mohamad, M.S. Takriff, (2010), Corros. Sci. 52, 3331
[14] E.M. Sherif, R.M. Erasmus, J.D. Comins, (2007), J. Colloid Interface Sci. 311, 144-157
[15] K.F. Khaled, S.A. Fadl-Allah, B. Hammouti, (2009), Mater. Chem. Phys. 117, 148-159
[16] A. Dandia, S. L. Gupta a, Sudheer, M. A. Quraishi, (2012), J. Mater. Environ. Sci. 3 (5), 993-1000
[17] Prasad, D. J.; Ashok, M.; Karegoudar, P.; Poojary, B.; Holla, B. S.; Sucheta, K. N., (2009), European Journal of Medicinal Chemistry 44, 551-567
[18] Almasirad, A. Tabatabai, S. A. Faizi, M. Kebriaeezadeh, A. Mehrabi, N. Dalvandi, A. Shafiee, A. (2004), Bioorganic & Medicinal Chemistry Letters, 14, 6057-6065
[19] M. Itoh, H. Nishihara, K. Aramaki, (1994), J. Electrochem. Soc. 141, 2018-2027
[20] Y. Yamamoto, H. Nishihara, K. Aramaki, (1993), J. Electrochem. Soc. 140, 436
[21] P. Udhayakala, T.V. Rajendiran, S. Gunasekaran, (2012), J Adv Sci Res, 3(3), 67-74
[22] A. Zarrouk, I. Warad, B. Hammouti, A. Dafali, S.S. Al-Deyab, N. Benchat, (2010), Int. J. Electrochem. Sci.5, 1516)
[23] Gaussian 09, Revision A.02, M. J. Frisch, G. W. Trucks, H. B. Schlegel, G. E. Scuseria, M. A. Robb, J. R. Cheeseman, G. Scalmani, V. Barone, B. Mennucci, G. A. Petersson, H. Nakatsuji, M. Caricato, X. Li, H. P. Hratchian, A. F. Izmaylov, J. Bloino, G. Zheng, J. L. Sonnenberg, M. Hada, M. Ehara, K. Toyota, R. Fukuda, J. Hasegawa, M. Ishida, T. Nakajima, Y. Honda, O. Kitao, H. Nakai, T. Vreven, J. A. Montgomery, Jr., J. E. Peralta, F. Ogliaro, M. Bearpark, J. J. Heyd, E. Brothers, K. N. Kudin, V. N. Staroverov, R. Kobayashi, J. Normand, K. Raghavachari, A. Rendell, J. C. Burant, S. S. Iyengar, J. Tomasi, M. Cossi, N. Rega, J. M. Millam, M. Klene, J. E. Knox, J. B. Cross, V. Bakken, C. Adamo, J. Jaramillo, R. Gomperts, R. E. Stratmann, O. Yazyev, A. J. Austin, R. Cammi, C. Pomelli, J. W. Ochterski, R. L. Martin, K. Morokuma, V. G. Zakrzewski, G. A. Voth, P. Salvador, J. J. Dannenberg, S. Dapprich, A. D. Daniels, O.

Farkas, J. B. Foresman, J. V. Ortiz, J. Cioslowski, and D. J. Fox, Gaussian, Inc., Wallingford CT, 2009.
[24] A.Zarrouk, H. Zarrok, R. Salghi, B. Hammouti1, S.S. Al-Deyab, R. Touzani, M. Bouachrine, I. Warad, T. B. Hadda, (2012), Int. J. Electrochem. Sci., 7, 6353–6364
[25] P. Udhayakalaa, A. Maxwell Samuelb, T. V. Rajendiranc and S. Gunasekarand, (2013), Der Pharmacia Lettre, 5 (2), 272-283
[26] C. Angeli, (1998), J. Chem. Ed., 75, 1494-1503
[27] Frank Jensen, (2007) Introduction to Computational Chemistry, Second Edition, John Wiley & Sons Ltd
[28] Charles A Mebi, (2011), J. Chem. Sci., 123, 727–731,
[29] Pearson R G., (1988), Inorg Chem, 27, 734-740
[30] M Elango, R Parthasarathi, G Karthik Narayanan, A Md Sabeelullah, U Sarkar, N S Venkatasubramaniyan, V Subramanian and P K Chattaraj, (2005), J. Chem. Sci., 117(1), 61-65
[31] P. Udhayakalaa, T.V. Rajendiranb and S. Gunasekaranc, (2012), Der Pharmacia Lettre, 4 (4), 1285-1298
[32] H. Shokry, R. Shah and E. M. Mabrouk, (2013), Journal of Advances in Chemistry, 5 (2), 702-718
[33] Parr RG, Yang W, (1984), J Am Chem Soc, 106, 4049-4058
[34] W. Yang, R. Parr, (1985) Proceedings of the National Academy of Sciences of the United States of America, 82, 6723–6726
[35] P. M. Niamien, F. K. Essy, A. Trokourey1, D. Sissouma, and D. Diabate, (2011), Afr. J. Environ. Sci. Technol, 5(9), 641-652
[36] Pengju Liu, Xia Fang, Yongming Tang, Chunning Sun, and Cheng Yao, (2011), Materials Sciences and Applications, 2, 1268-1278,
[37] Huiwen Tian, Weihua Li, Baorong Hou, (2013), Int. J. Electrochem. Sci., 8, 8513-8529
[38] Gomez B, Likhanova NV, Dominguez-Aguilar MA, Martinez-Palou R Vela A, Gasquez J., J Phy Chem, 110, 2006; 8928-8934
[39] P.Udhayakala1, T.V. Rajendiran and S. Gunasekaran, J. Chem. Bio. Phy. Sci. Sec.A, 2(3), 2012, 1151-1165
[40] N. Boussalah, S. Ghalem, S. El Kadiri, B. Hammouti, and R. Touzani, (2008), Res Chem Intermed, 34,
[41] Suban K. Sahoo, Darshna Sharma, Rati Kanta Bera, (2012), J Mol Model, 18, 1993–2001
[42] Reza Ghiasi and Allieh Boshak, (2013), J. Mex. Chem. Soc. 57(1), 8-15,
[43] Reza Ghiasi and Hoda Pasdar, (2013), Russian Journal of Physical Chemistry A, 87(6), 973–978,